Measurements of Higgs boson decaying into tau leptons using 139 fb^{-1} at the ATLAS experiment

Antonio De Maria
HuanguoLi

Nanjing University

November 25, 2021

- Lagrangian of the SM Higgs boson couplings with SM particles

$$\mathcal{L} = -\frac{m_f}{v} f\bar{f}H + \frac{m_H^2}{2v}H^3 + \frac{m_H^2}{8v^2}H^4 + \delta_V V_\mu V^\mu \left(\frac{2m_V^2}{v}H + \frac{m_V^2}{v^2}H^2\right)$$

- Coupling with SM particles proportional to:
  - m_F for fermions → mainly coupling with third generation of quark and leptons (b and τ)
  - m_V^2 for bosons → mainly coupling with W and Z
- In the SM, $H \to \tau\tau$ is the important accessible decay at LHC to establish Higgs Yukawa coupling to leptons

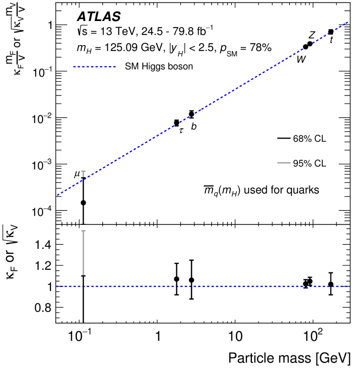

Phys. Rev. D 101 (2020) 012002

$H \to \tau\tau$ Measurements - ATLAS-CONF-2021-044

Production modes

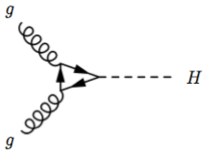

gluon fusion (ggF)

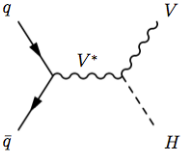

associated production with a gauge boson (VH)

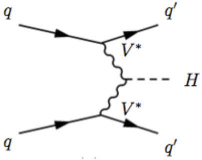

vector boson fusion (VBF)

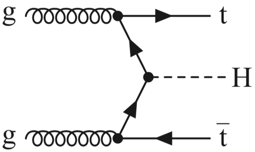

associated production with a $t\bar{t}$ pair (ttH)

Di-tau decay modes combination

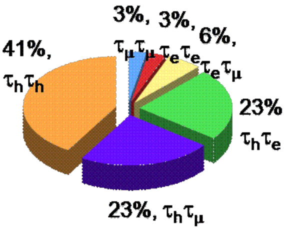

Single τ Decay Mode	BR (%)
$\mu^\pm$	17.4
$e^\pm$	17.4
$h^\pm$	11.5
$h^\pm\pi^0$	30.0
$h^\pm \geqslant 2\pi^0$	10.6
$3h^\pm$	9.5
$3h^\pm \geqslant 2\pi^0$	5.1

- Latest publication using full Run-2 dataset
- Consider the main Higgs boson production modes
- Take all di-tau decay modes combination into account

Tau Reconstruction/Identification

- Attempt to reconstruct hadronically decay taus
- Tau candidates are seeded by anti-k_t LC jets with a distance parameter R = 0.4
- Identification algorithm based on RNN to reject background from q/g jets
  - RNN trained using track and cluster information
  - highly improved performance compared with BDT based identification

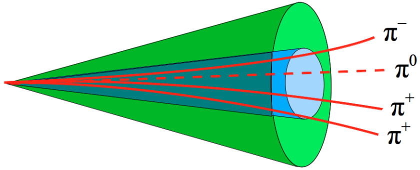

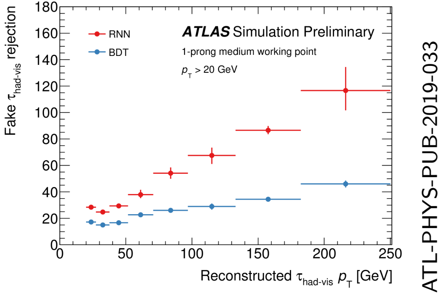

Analysis Categorisation and Background Estimation

	$\tau_{lep}\tau_{lep}$	$\tau_{lep}\tau_{had}$	$\tau_{had}\tau_{had}$
VBF inclusive	sub-leading jet $p_T > 30$ GeV $m_{jj} > 350$ GeV, $\lvert\Delta\eta_{jj}\rvert > 3$ $\eta(j_0)\times\eta(j_1) < 0$ lepton centrality: visible decay products of the τ leptons between VBF jets		
VH inclusive	$60\,\text{GeV} < m_{jj} < 120\,\text{GeV}$ sub-leading jet $p_T > 30$ GeV		
tt(0L)$H \to \tau_{had}\tau_{had}$			# of jets ≥ 6 and # of b-jets ≥ 1 or # of jets ≥ 5 and # of b-jets ≥ 2
Boost inclusive	Not VBF inclusive Not VH inclusive $p_T(H) > 100$ GeV		

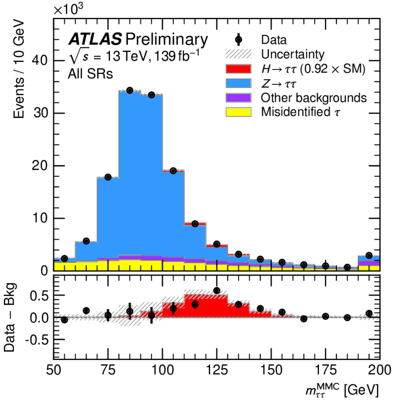

- Z$\to \tau\tau$ (70-90%) : MC based and validated + normalised using embedded Z$\to$ *ll* CRs
- Misidentified τ (5-20 %) : Data-driven estimated using Matrix Method ($\tau_{lep}\tau_{lep}$) and Fake Factor Method ($\tau_{lep}\tau_{had}$ and $\tau_{had}\tau_{had}$)
- Other backgrounds : small, evaluated through MC

Kinematic Embedding Procedure

- Select Z$\rightarrow$ *ll* + jets events in CRs defined orthogonal to the signal region
- Unfold Z$\rightarrow$ *ll* events taking into account lepton reconstruction efficiencies
- Mimic Z$\rightarrow \tau\tau$ events through kinematic parameterisation of τ decay products
- Procedure validated in different kinematic phase spaces

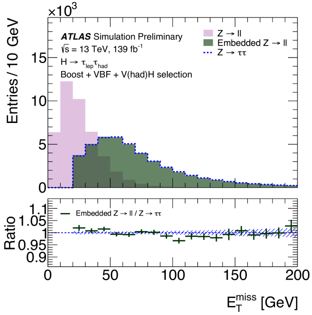

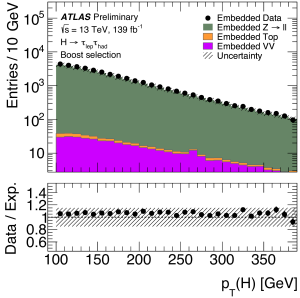

Misidentified τ Background Estimation

- Aim to estimate jet mis-identified as τ (light leptons) in $\tau_{lep}\tau_{had}$ and $\tau_{had}\tau_{had}$ ($\tau_{lep}\tau_{lep}$) final states
- Validated in dedicated CRs and residual mis-modelling assigned as systematic uncertainty

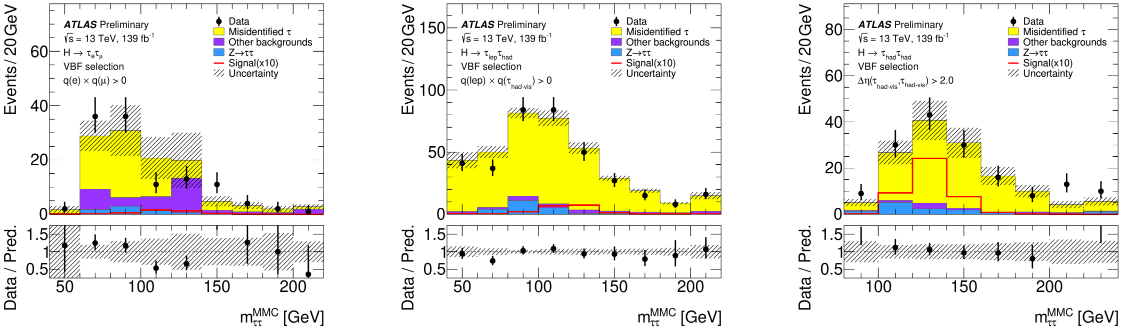

Fit Model

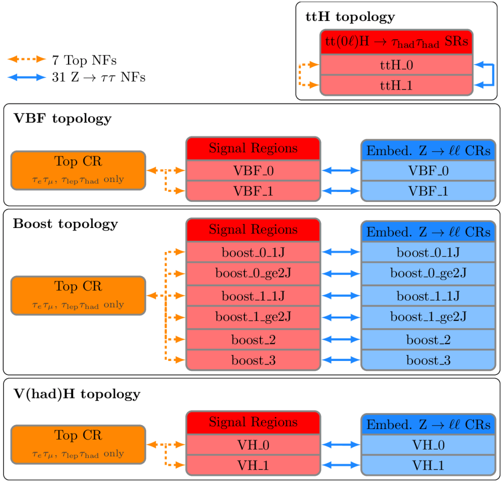

- Use di-τ mass (MMC) as fit variable in the SRs
- VBF, VH(had) and ttH signal regions split using taggers
- Boost region split according to the kinematics
- Use embedded Z$\rightarrow$ ll (Top) CRs to normalize Z$\rightarrow \tau\tau$ (Top) background

Postfit Distributions

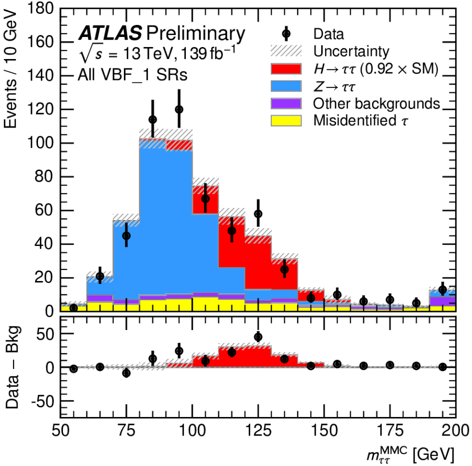

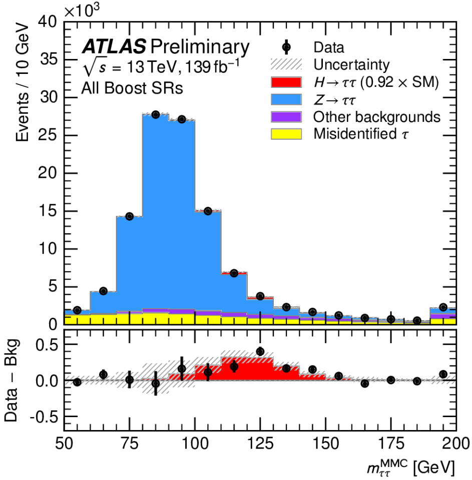

- Clear signal excess over background prediction in the most sensitive region

Inclusive Cross-section Measurement

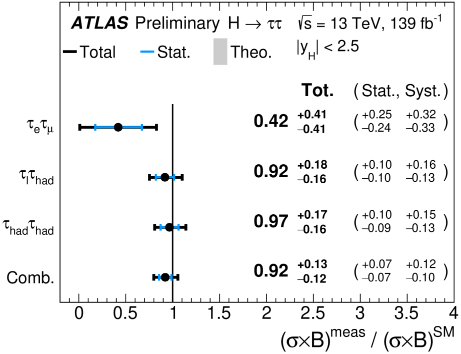

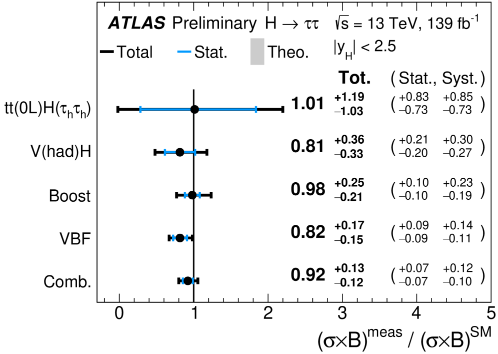

- Largest sensitivity from $\tau_{lep}\tau_{had}$ and $\tau_{had}\tau_{had}$ final states and VBF and Boost categories
- Total uncertainty $\simeq$ 13%; nearly twice improvement respect to previous publication
- Uncertainty dominated by systematic component mainly from Theory, Jet/E_T^{miss} and MC sample statistics

Production Mode Measurement Results

- Observation of the VBF H$\rightarrow \tau\tau$ with significance of 5.3 (6.2) σ observed (expected)
- Evidence of the ggH H$\rightarrow \tau\tau$ with significance of 3.9 (4.6) σ observed (expected)
- All the measurements in agreement with SM prediction

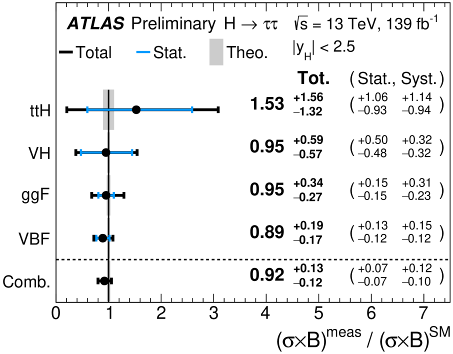

STXS Measurement Results

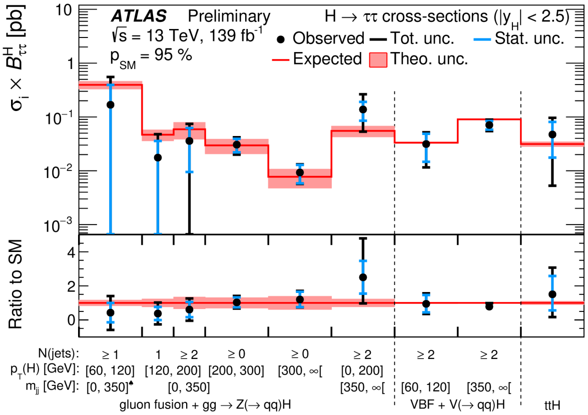

- Measurement performed in 9 STXS bins divided by p_T^H and jet kinematics
- Largest sensitivity from ggH with high p_T^H and VBF bins

Summary

- The most recent measurements in the H$\rightarrow \tau\tau$ channel have been presented
- Aim was to measure the inclusive, production mode and STXS bins cross-sections
- Inclusive cross-section measured with $\simeq$ 13% uncertainty and in agreement with SM prediction
  - uncertainty by systematic uncertainty from Theory, Jet/E_T^{miss} and MC sample statistics
- Observation (evidence) of the VBF (ggH) production mode with observed significance of 5.3 (3.9) σ
- Cross-section measured also in 9 STXS bins with best results from ggH with high p_T^H and VBF bins

Thanks For Your Attention

Backup

Higgs Boson Production Modes

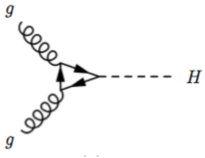

gluon fusion (ggF)
Cross section : 48.6 pb.*

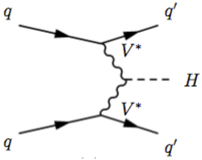

vector boson fusion (VBF).
Cross section : 3.8 pb.*

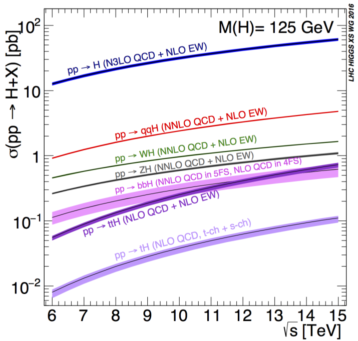

Higgs boson production cross section

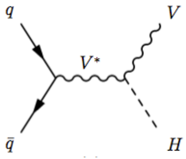

associated production with a gauge boson (VH).
Cross section : 2.3 pb.*

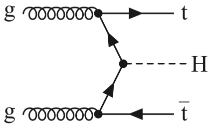

associated production with a $t\bar{t}$ pair (ttH).
Cross section : 0.5 pb.*

* predicted cross section for m_H=125 GeV at $\sqrt{s}$=13 TeV

Higgs Boson Decay Branching Ratios

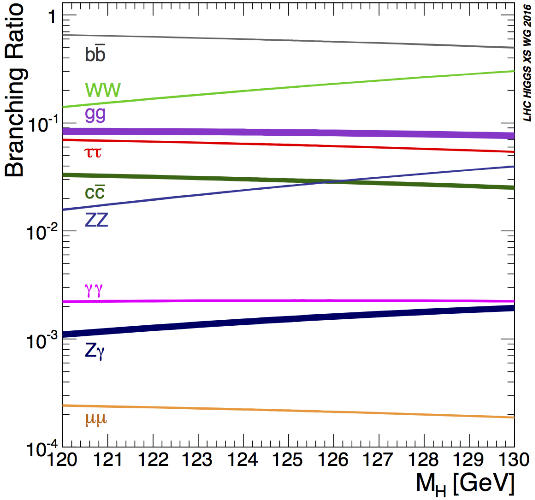

- Larger branching ratio (BR) for $H \to b\bar{b}$, $H \to WW^*$ and $H \to \tau\tau$, however poor mass resolution and large background contamination
- $H \to \gamma\gamma$ and $H \to ZZ^*(\to 4l)$ have lower BR, but high mass resolution; can be used for precision measurements
- $H \to Z\gamma$ and $H \to \mu\mu$ becoming now accessible thanks to large Run 2 dataset and the good detector performance

Measurement Uncertainties

Source of uncertainty	Impact on $\Delta\sigma / \sigma(pp \to H \to \tau\tau)$ [%] Observed	Expected
Theoretical uncertainty in signal	8.1	8.6
Jet and $\vec{E}_{\mathrm{T}}^{\mathrm{miss}}$	4.2	4.1
Background sample size	3.7	3.4
Hadronic τ decays	2.0	2.1
Misidentified τ	1.9	1.8
Luminosity	1.7	1.8
Theoretical uncertainty in Top processes	1.4	1.2
Theoretical uncertainty in Z+jets processes	1.1	1.1
Flavor tagging	0.5	0.5
Electrons and muons	0.4	0.3
Total systematic uncertainty	11.1	11.0
Data sample size	6.6	6.3
Total	12.8	12.5

- Total uncertainty $\simeq$ 13%; $\simeq$ factor 2 improvement respect to previous publication
- Uncertainty dominated by systematic component
- Largest source of uncertainty from Theory, Jet/E_T^{miss} and MC sample statistics

Production and STXS Measurement

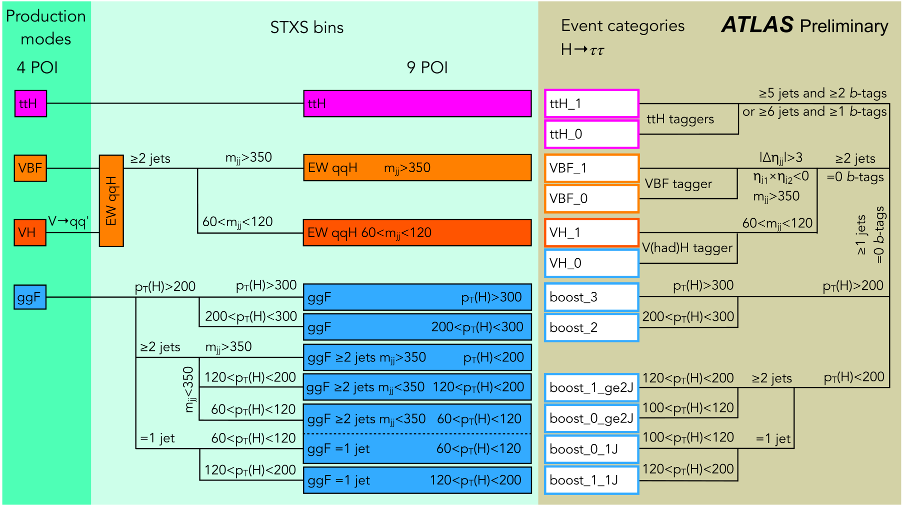

- STXS bins definition: maximize sensitivity, minimize theory dependence
- Bins defined to enrich events of certain production mode

STXS Measurement Results

STXS bin				SM prediction	Result	Stat. unc.	Syst. unc. [pb]		
Process	m_{jj} [GeV]	$p_{\mathrm{T}}(H)$ [GeV]	$\mathrm{N_{jets}}$	[pb]	[pb]	[pb]	Th. sig.	Th. bkg.	Exp.
$\mathrm{ggF} + gg \to Z(\to qq)H$	$[0,\ 350]^{\spadesuit}$	$[60,\ 120]$	≥ 1	0.39 ± 0.06	0.17 ± 0.39	± 0.22	± 0.06	± 0.15	± 0.29
		$[120,\ 200]$	$= 1$	0.047 ± 0.011	0.018 ± 0.030	± 0.018	± 0.004	± 0.004	± 0.019
	$[0,\ 350]$	$[120,\ 200]$	≥ 2	0.059 ± 0.020	0.036 ± 0.039	± 0.027	± 0.009	± 0.009	± 0.025
		$[200,\ 300]$	≥ 0	0.030 ± 0.009	0.031 ± 0.011	± 0.009	± 0.003	± 0.001	± 0.006
		$[300,\ \infty[$	≥ 0	0.008 ± 0.003	0.009 ± 0.004	± 0.003	± 0.001	± 0.000	± 0.001
	$[350,\ \infty[$	$[0,\ 200]$	≥ 2	0.055 ± 0.013	0.14 ± 0.11	± 0.05	± 0.06	± 0.01	± 0.07
EWK	$[60, 120]$		≥ 2	0.033 ± 0.001	0.031 ± 0.020	± 0.017	± 0.003	± 0.001	± 0.010
	$[350,\ \infty[$		≥ 2	0.090 ± 0.002	0.071 ± 0.017	± 0.014	± 0.010	± 0.002	± 0.006
$t\bar{t}H$				0.031 ± 0.003	0.047 ± 0.046	± 0.032	± 0.011	± 0.027	± 0.018